

Rapid evolution of the most luminous galaxies during the first 900 million years

Rychard J. Bouwens¹ & Garth D. Illingworth¹

The first 900 million years (Myr) to redshift $z \approx 6$ (the first seven per cent of the age of the Universe) remains largely unexplored for the formation of galaxies. Large samples of galaxies have been found at $z \approx 6$ (refs 1–4) but detections at earlier times are uncertain and unreliable. It is not at all clear how galaxies built up from the first stars when the Universe was about 300 Myr old ($z \approx 12$ –15) to $z \approx 6$, just 600 Myr later. Here we report the results of a search for galaxies at $z \approx 7$ –8, about 700 Myr after the Big Bang, using the deepest near-infrared and optical images ever taken. Under conservative selection criteria we find only one candidate galaxy at $z \approx 7$ –8, where ten would be expected if there were no evolution in the galaxy population between $z \approx 7$ –8 and $z \approx 6$. Using less conservative criteria, there are four candidates, where 17 would be expected with no evolution. This demonstrates that very luminous galaxies are quite rare 700 Myr after the Big Bang. The simplest explanation is that the Universe is just too young to have built up many luminous galaxies at $z \approx 7$ –8 by the hierarchical merging of small galaxies.

High-redshift galaxies can be identified using the well-established “dropout” technique⁵. Absorption shortward of 91.2 nm and 121.6 nm by intervening neutral hydrogen results in a sharp change (a break) in the spectral energy distribution in redshifted galaxies and can be used to determine their redshift⁶. In the three years since the first galaxies were discovered in the reionization epoch^{7,8} using this dropout technique, 500 galaxies¹ are now known at $z \approx 6$ and the frontier for exploration has shifted to galaxies at $z \approx 7$ –8 and higher redshifts. Finding galaxies at redshifts beyond $z \approx 6$ is very challenging, however, because the sources are extremely faint, and the high sky backgrounds make ground-based searches in the near-infrared part of the spectrum very difficult. Although near-infrared imaging from space largely overcomes this problem, we are limited by the areal coverage of the available instrumentation. For example, the Hubble Space Telescope (HST) Near Infrared Camera and Multi-object Spectrograph (NICMOS) instrument⁹—the only near-infrared imaging instrument in space—has a very small field of view (0.8 arcmin²), which is just 7% of the area of the optical camera on HST, the Advanced Camera for Surveys (ACS). This has made it extremely time-consuming to survey large areas of sky for high-redshift sources.

Nonetheless, we were able to use the deep near-infrared NICMOS data over the Hubble Ultra Deep Field (HUDF)¹⁰ to conduct the first significant search for $z \approx 7$ –8 galaxies^{3,11}. The few candidates found were consistent with a slight increase in the volume density of luminous sources from $z \approx 7$ –8 to $z \approx 6$ (from 700 Myr to 900 Myr after the Big Bang). However, owing to possible instrumental problems for some of the candidates and the large uncertainty caused by large-scale structure effects, we were not able to draw very strong conclusions about the evolution of the luminosity function, the ultraviolet (UV) luminosity density, and the star-formation rate

from $z \approx 7$ –8 to $z \approx 6$. Attempts to establish these quantities based on other data sets have also been quite uncertain¹².

Fortunately, sufficient NICMOS and ACS data are now available that we can firmly establish the density of luminous galaxies at $z \approx 7$ –8 and the evolution with respect to $z \approx 6$. These data come from many years of primary and parallel observations with HST and include $> \sim 20$ arcmin² of deep NICMOS data (reaching J and H band limits of ~ 27 –28 AB mag at 5σ) that overlap with HST ACS data of comparable depth. A substantial fraction of these data are available over the two Great Observatories Origins Deep Survey fields¹³ and permit a much more robust search for $z \approx 7$ –8 galaxies than was possible with the HUDF data alone—significantly increasing our search area and allowing us to average over the effects of large-scale structure. The search fields used for our $z \approx 7$ –8 selection are given in Supplementary Fig. 1 and Supplementary Table 1^{10,13–15}. These extensive ACS and NICMOS data sets were processed using recently developed reduction software¹⁶ (R.J.B. *et al.*, manuscript in preparation). After registration of these data onto the same frame, object catalogues were generated with SExtractor¹⁷ from all 4σ detections found in a χ^2 image (generated from the J and H images). These catalogues were cleaned of spurious or other marginal detections by requiring objects to be 4.5σ in the H band (0.3" diameter aperture) and the photometry performed, after smoothing the images to a consistent point spread function.

We then considered two different z-dropout selections on these catalogues. z-dropout selections identify star-forming galaxies at $z \approx 7$ –8 that show a strong flux break between the z and J bands due to the 121.6 nm absorption feature, but have very blue infrared colours (see Supplementary Fig. 2). Our first selection was a relatively conservative one that was designed to isolate a robust set of z-dropouts. Our second selection was a little more aggressive and designed to find a larger sample of candidates (albeit less secure) and to test the robustness of the results derived from our first selection. Applying these criteria to our photometric catalogues, only one z-dropout candidate made our conservative selection and four candidate z-dropouts made our less-conservative selection. There were two other sources in our search fields that satisfied our selection criteria, but they are very likely to be T-dwarf stars. All four $z \approx 7$ –8 candidates are shown in Fig. 1 and their properties are listed in Supplementary Table 2. A detailed discussion of our current selection is provided in the Supplementary Information.

What do these z-dropout candidates imply for the evolution of the rest-frame UV luminosity function? (The UV luminosity function describes the number density of the galaxies versus the UV luminosity and is usually parameterized as $\phi^* e^{-L/L^*} (L/L^*)^\alpha$ where ϕ^* is the normalization of the galaxy population, L^* is the characteristic luminosity of the galaxy population, and α is the faint-end slope of the galaxy population.) We compared the current numbers with what we might have expected if galaxies at $z \approx 7$ –8 were similar to those at

¹UCO/Lick Observatory and Department of Astronomy, University of California Santa Cruz, Santa Cruz, California 95064, USA.

$z \approx 6$, just 200 million years later. We can compute the expected number by using our cloning software to artificially redshift the $z \approx 6$ population over the redshift range of our sample, add them to our data, and then repeat the selection^{18,19}. We estimated that we would find 10.1 ± 3.5 z -dropouts using our conservative selection and 17.0 ± 4.9 z -dropouts using our less conservative selection. This is clearly substantially more than the 1 and 4 z -dropout candidates found in our conservative and less-conservative selections, respectively, which suggests that there has been substantial evolution for galaxies that lie at the bright end of the luminosity function. For simple poissonian statistics, the present samples are inconsistent with no evolution in the galaxy population between $z \approx 7-8$ and $z \approx 6$, at 99.90% and 99.93% confidence, respectively.

To make a proper assessment of the significance of this result, however, we need to account for the effects of galaxy clustering ('large-scale structure'). Modelling the selection volume in our individual fields with a window of depth $\Delta z = 1$ at $z \approx 7-8$ and bias of 7 (see Supplementary Information for details), we estimate the

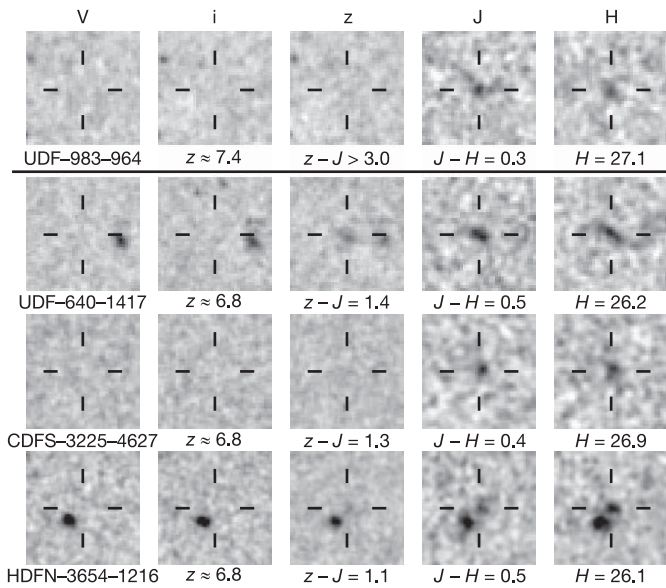


Figure 1 | Optical and near-infrared images of four candidate galaxies at $z \approx 7-8$. The uppermost candidate is the only object satisfying our most conservative z -dropout criterion ($z_{850} - J_{110} > 1.3$, $z_{850} - J_{110} > 1.3 + 0.4(J_{110} - H_{160})$, $J_{110} - H_{160} < 1.2$, undetected [$<2\sigma$] in the V_{606} and i_{775} bands). This object is undetected ($<2\sigma$) in the extremely deep optical B-V-i-z data available in the HUDF, has a $z_{850} - J_{110}$ colour redder than 3.0 mag (1σ), and a $J_{110} - H_{160}$ colour of 0.3 mag. It also shows a significant 5σ detection in the InfraRed Array Channel (IRAC) 3.6- μm and 4.5- μm coverage (M. Dickinson *et al.*, manuscript in preparation) that we have from the Spitzer Space Telescope³¹, with optical-infrared colours very similar to dropouts found at $z \approx 6$ (refs 23–26). While this object lacks spectroscopic confirmation (and will probably continue to do so, because it is so faint), it seems extremely probable that it is at $z \approx 7-8$. It had previously been reported as a z -dropout candidate in the HUDF¹¹. The lower three candidates satisfy our less-conservative z -dropout criterion ($z_{850} - J_{110} > 0.8$, $z_{850} - J_{110} > 0.8 + 0.4(J_{110} - H_{160})$, $J_{110} - H_{160} < 1.2$, undetected [$<2\sigma$] in the V_{606} and i_{775} bands). Though each of these sources is consistent with being at the low-redshift edge of the selection ($z \approx 6.8$), the optical imaging available for two of these sources (CDFS-3225-4627 and HDFN-3654-1216) is not deep enough to completely rule out their being low-redshift sources (or T-dwarf stars in the case of CDFS-3225-4627). All z -dropout candidates considered here were detected at $>4\sigma$ and $>4.5\sigma$ in the J and H bands, respectively, and were found in NICMOS data with at least seven individual exposures. The V, i, z, J and H images shown here correspond to the ACS F606W, ACS F775W, ACS F850LP, NICMOS F110W, and NICMOS F160W filters, respectively, with central wavelengths of 591, 776, 944, 1,119 and 1,604 nm, respectively. Each cutout is $3.5'' \times 3.5''$ in size.

field-to-field variance to be $\sim 41\%$ and $\sim 49\%$ for our ~ 5 -arcmin² fields and 0.8-arcmin² fields, respectively^{20,21}. Including the effect of large-scale structure increases the uncertainties on our expected numbers, that is, $10.1_{-5.0}^{+3.1}$ sources with our conservative search and $17.0_{-7.2}^{+4.7}$ sources for our less-conservative search. Again, this is inconsistent with no galaxy evolution, at 99.5% and 99.4% confidence, respectively, and indicates a dramatic drop in the overall prevalence of luminous galaxies over this short time interval. We estimate that the number density of luminous galaxies at $z \approx 7-8$ is just $0.10_{-0.07}^{+0.19}$ times that at $z \approx 6$ for our conservative search and $0.24_{-0.12}^{+0.20}$ times the $z \approx 6$ value for our less-conservative selection. The two determinations here are consistent within the errors and suggest that our basic result is robust. For simplicity, we will use statistics from our more rigorous, conservative search for the remainder of this paper.

What does this deficit of luminous star-forming objects at $z \approx 7-8$ tell us about evolution of the UV luminosity function? This deficit could be due to a change in the overall number density of galaxies or due to a change in luminosity of the brightest objects (or some combination thereof). Perhaps the simplest and most natural explanation, though, is through an evolution of the characteristic luminosity L^* . It is already well established that L^* brightens significantly over the interval $z \approx 6$ to $z \approx 3$ (Fig. 2)^{11,2}, so it seems reasonable to

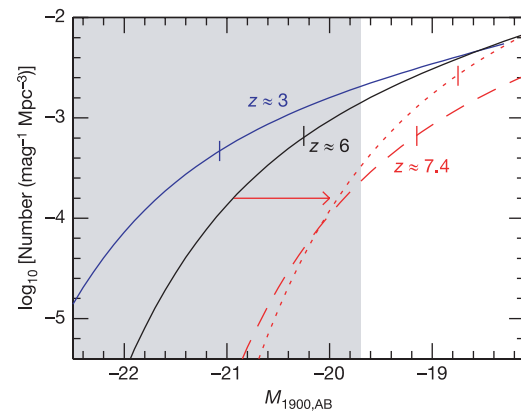


Figure 2 | UV luminosity functions at redshift $z \approx 3, 6$ and 7.4 . The red lines show two possible luminosity functions at $z \approx 7-8$ that are consistent with the surface density of $z \approx 7-8$ galaxies (z -dropouts). These luminosity functions are compared with existing $z \approx 6$ and $z \approx 3$ luminosity functions^{1,29}. The characteristic luminosity for each luminosity function is indicated on the figure with a short vertical line. The grey region shows the approximate flux range of the current z -dropout study. The luminosity functions here are plotted in terms of the number of galaxies per magnitude per cubic megaparsec and are a function of the absolute magnitude of galaxies (M_{AB}) at 1900 Å. The rest-frame UV luminosity functions brightens considerably from $z \approx 6$ to $z \approx 3$ (refs 1, 2), and it seems reasonable to imagine that this trend continues from even earlier times (that is, from $z \approx 7-8$ to $z \approx 6$). The first luminosity function (dashed line) was obtained by requiring the $z \approx 7-8$ luminosity function to have the same normalization ϕ^* and faint-end slope α as the luminosity function at $z \approx 6$ (solid black line)¹, but changing the characteristic luminosity L^* to match the observed surface density of $z \approx 7-8$ galaxies. The second luminosity function (dotted line) was obtained by requiring the product of ϕ^* and L^* to be a constant (to maintain an approximately constant luminosity density), fixing α to the $z \approx 6$ value ($\alpha = -1.73$), but changing the characteristic luminosity L^* to match observed surface density of $z \approx 7-8$ galaxies. The characteristic luminosity which best fits our search results is 1.1 ± 0.4 mag fainter than the $z \approx 6$ value for the first luminosity function and 1.5 ± 0.4 mag fainter for the second luminosity function (equivalent to $H_{160,AB}$ -band magnitudes of 28.0 ± 0.4 mag and 28.4 ± 0.4 mag, respectively). This best-fit characteristic luminosity is 0.1 mag fainter and 0.1 mag brighter assuming faint-end slopes α of -1.4 and -2.0 , respectively. The 'concordance' cosmology ($\Omega_m = 0.3$, $\Omega_\Lambda = 0.7$, $H_0 \approx 70 \text{ km s}^{-1} \text{ Mpc}^{-1}$) is assumed in this figure and in Fig. 3.

imagine that this trend continues from $z \approx 7-8$ to $z \approx 6$. A relevant question to ask is how much fainter the characteristic luminosity at $z \approx 7-8$ would need to be to reproduce the observed decline. There are two obvious ways to model this change: (1) vary L^* while keeping the normalization $\phi^* = 0.002 \text{ Mpc}^{-3}$ and faint-end slope $\alpha = -1.73$ fixed at the $z \approx 6$ values and (2) vary L^* while keeping the product of ϕ^* and L^* fixed (and α fixed) to maintain a constant luminosity density at $z \geq 6$. The latter model is motivated by a number of recent results at high redshift, which suggest that the rest-frame UV luminosity density—and the total star-formation rate density—shows very mild evolution^{1,22}. These latter observations include the high stellar masses found in many $z \approx 5-6$ systems and large optical depths measured by the Wilkinson Microwave Anisotropy Probe ($\tau = 0.09 \pm 0.03$), both of which suggest substantial high-redshift ($z > 6$) star formation²³⁻²⁸. For the above models, we can evaluate the evolution in the characteristic luminosity needed to

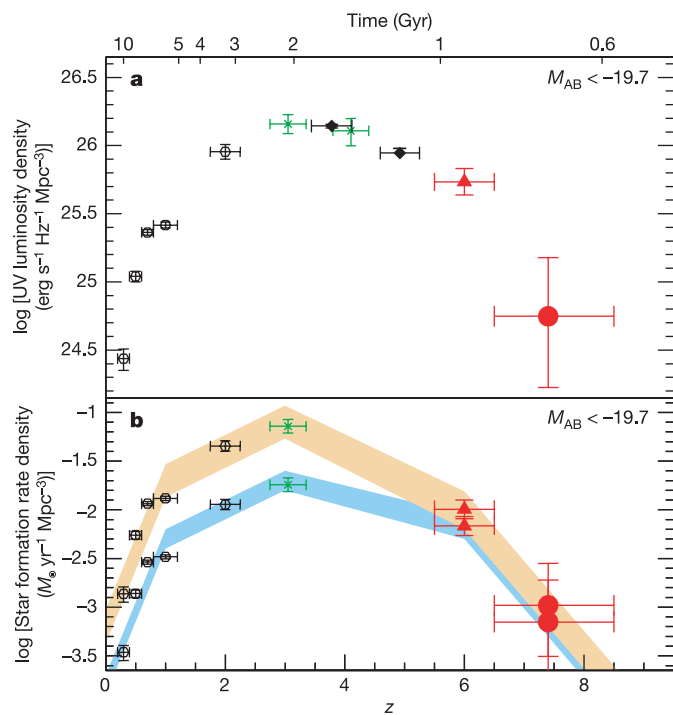


Figure 3 | The luminosity density and star-formation rate density of the Universe over time. **a**, The UV luminosity density at $1,900 \text{ \AA}$ from $z \approx 0$ to $z \approx 7-8$. Because of the flux limits of the current z -dropout searches, we plot the luminosity densities only down to a flux limit of $M_{\text{AB}} \approx -19.7$ mag (which is equivalent to 0.6 times the characteristic luminosity at $z = 6$)¹. The new determination is shown as a large filled circle at $z \approx 7.4$ (with 1σ errors that include both poissonian and large-scale structure uncertainties) and compared with determinations at $z \approx 0-2$ (open hexagons)³⁰, $z \approx 3$ (green crosses)²⁹, $z \approx 4-5$ (black diamonds)²², and $z \approx 6$ (red triangle)¹. Vertical error bars on the latter determinations are all 1σ while the horizontal error bars show the approximate redshift range of applicability. The luminosity density shows an abrupt increase from $z \approx 7-8$ to $z \approx 6$, indicating that there has been a rapid build-up in luminous galaxies (those >0.6 times the characteristic luminosity at $z = 6$, that is, $>0.6L^*_{z=6}$) over this range in redshift—which corresponds to a period of just 200 million years. **b**, The star-formation-rate history of the Universe shown with and without a correction for dust extinction (upper and lower points, respectively). The errors on the points are the same as in **a**. This star-formation-rate history is plotted in terms of the number of solar-mass stars forming per year per unit comoving megaparsec and is derived here from the UV luminosity densities assuming a Salpeter initial mass function, which extends from $0.1 M_{\odot}$ to $100 M_{\odot}$, where M_{\odot} is the mass of the Sun³². To account for the apparent evolution in the UV colours and thus the dust properties of high-redshift galaxies^{1,26,33}, we apply more minimal (~ 0.4 mag) dust corrections at $z > 5$, but revert to more standard values (~ 1.4 mag) at $z \leq 3$ (ref. 30).

produce the factor-of-ten deficit in luminous galaxies at $z \approx 7-8$ by repeating the Monte Carlo simulations described above. The end result is that we find that the characteristic luminosity at $z \approx 7-8$ in the rest-frame UV ($\sim 1,900 \text{ \AA}$) must be 1.1 ± 0.4 mag fainter than $z \approx 6$ to reproduce the observed result for our first set of assumptions and 1.5 ± 0.4 mag fainter for our second (see Fig. 2). In both cases, the evolution is fairly dramatic and suggests that most galaxies at $z \approx 7-8$ are much fainter than our survey limits.

The evolution observed here can best be presented in the terms of the rest-frame continuum UV luminosity density integrated down to our approximate magnitude limit $M_{\text{AB}} \approx -19.7$ mag and compared with similar determinations at other redshifts (Fig. 3)^{1,22,29,30}. As is evident from Fig. 3, the luminosity density, and especially the star-formation rate (the extinction-corrected luminosity density), increases rapidly at early times and indicates that there is a rapid build-up in the most-luminous systems that continues from $z \approx 7-8$ (700 Myr) to $z \approx 4$ (1,600 Myr).

The simplest explanation for this large deficit of the most luminous galaxies at $z \approx 7-8$ relative to that at $z \approx 6$, just 200 Myr later, is that the Universe is simply too young to have built up many luminous systems, and that the majority of galaxies at $z \approx 7-8$ have luminosities much fainter than $M_{\text{AB}} \approx -19.7$ mag. Hierarchical build-up would suggest such a result, but detailed modelling is needed to establish whether the rate of change measured here is consistent. Determining the nature of the $z \approx 7-8$ star-forming population will be a challenge, requiring significantly deeper observations. The HST Wide-Field Camera 3 will provide a near-term opportunity, but ultimate elucidation of the galaxy buildup in the first 500 Myr awaits the James Webb Space Telescope.

Received 6 April; accepted 1 August 2006.

- Bouwens, R. J., Illingworth, G. D., Blakeslee, J. P. & Franx, M. Galaxies at $z \sim 6$: The UV luminosity function and luminosity density from 506 UDF, UDF-Ps, and GOODS i-dropouts. *Astrophys. J.* (in the press); preprint at (<http://www.arXiv.org/astro-ph/0509641>) (2005).
- Dickinson, M. *et al.* Color-selected galaxies at $z \sim 6$ in the great observatories origins deep survey. *Astrophys. J.* **600**, 99–102 (2004).
- Yan, H. J. & Windhorst, R. A. Candidates of $z \sim 5.5-7$ galaxies in the Hubble Space Telescope Ultra Deep Field. *Astrophys. J.* **612**, 93–96 (2004).
- Bunker, A. J., Stanway, E. R., Ellis, R. S. & McMahon, R. G. The star formation rate of the Universe at $z \sim 6$ from the Hubble Ultra Deep Field. *Mon. Not. R. Astron. Soc.* **355**, 374–384 (2004).
- Steidel, C. C., Gialalisco, M., Pettini, M., Dickinson, M. & Adelberger, K. L. Spectroscopic confirmation of a population of normal star-forming galaxies at redshifts $Z > 3$. *Astrophys. J.* **462**, 17–20 (1996).
- Madau, P. Radiative transfer in a clumpy universe: The colors of high-redshift galaxies. *Astrophys. J.* **441**, 18–27 (1995).
- Becker, R. H. *et al.* Evidence for reionization at $z \sim 6$: detection of a Gunn-Peterson trough in a $z = 6.28$ quasar. *Astron. J.* **122**, 2850–2857 (2001).
- Fan, X. *et al.* Evolution of the ionizing background and the epoch of reionization from the spectra of $z \sim 6$ quasars. *Astronom. J.* **123**, 1247–1257 (2002).
- Skinner, C. J. *et al.* On-orbit properties of the NICMOS detectors on HST. *Proc. SPIE* **3354**, 2–13 (1998).
- Thompson, R. I. *et al.* The Near-Infrared Camera and Multi-Object Spectrometer Ultra Deep Field: observations, data reduction, and galaxy photometry. *Astron. J.* **130**, 1–12 (2005).
- Bouwens, R. J. *et al.* Galaxies at $z \sim 7-8$: z_{850} -dropouts in the Hubble Ultra Deep Field. *Astrophys. J.* **616**, 79–82 (2004).
- Richard, J., Pello, R., Schaerer, D., Le Borgne, J.-F. & Kneib, J.-P. Constraining the population of $6 < z < 10$ star-forming galaxies with deep near-IR images of lensing clusters. *Astron. Astrophys.* (in the press); preprint at (<http://www.arXiv.org/astro-ph/0606134>) (2006).
- Gialalisco, M. *et al.* The Great Observatories Origins Deep Survey: initial results from optical and near-infrared imaging. *Astrophys. J.* **600**, 99–102 (2004).
- Thompson, R. I. *et al.* Near-Infrared Camera and Multi-Object Spectroscopic observations of the Hubble Deep Field: observations, data reduction, and galaxy photometry. *Astron. J.* **117**, 17–39 (1999).
- Dickinson, M. A. Complete NICMOS map of the Hubble Deep Field North. *AIP Conf. Proc.* **470**, 122–132 (1999).
- Blakeslee, J. P., Anderson, K. R., Meurer, G. R., Benítez, N. & Magee, D. An automatic image reduction pipeline for the Advanced Camera for Surveys. in *Astronomical Data Analysis Software and Systems XII* (eds Payne, H. E., Jedrzejewski, R. I. & Hook, R. N.) 257–260 (ASP Conf. Ser. 295, Astronomical Society of the Pacific, 2003).

17. Bertin, E. & Arnouts, S. SExtractor: software for source extraction. *Astron. Astrophys.* **117** (Suppl.), 393–404 (1996).
18. Bouwens, R. J., Broadhurst, T. J. & Silk, J. Cloning Hubble Deep Fields. I. A model-independent measurement of galaxy evolution. *Astrophys. J.* **506**, 557–578 (1998).
19. Bouwens, R. J., Broadhurst, T. J. & Illingworth, G. D. Cloning dropouts: implications for galaxy evolution at high redshift. *Astrophys. J.* **593**, 640–660 (2003).
20. Mo, H. J. & White, S. D. M. An analytic model for the spatial clustering of dark matter haloes. *Mon. Not. R. Astron. Soc.* **282**, 347–361 (1996).
21. Somerville, R. S. *et al.* Cosmic variance in the Great Observatories Origins Deep Survey. *Astrophys. J.* **600**, 171–174 (2004).
22. Giavalisco, M. *et al.* The rest-frame ultraviolet luminosity density of star-forming galaxies at redshifts $z > 3.5$. *Astrophys. J.* **600**, 103–106 (2004).
23. Eyles, L. *et al.* Spitzer imaging of *i'*-drop galaxies: old stars at $z \sim 6$. *Mon. Not. R. Astron. Soc.* **364**, 443–454 (2005).
24. Yan, H. *et al.* Rest-frame ultraviolet-to-optical properties of galaxies at $z \sim 6$ and 5 in the Hubble Ultra Deep Field: from Hubble to Spitzer. *Astrophys. J.* **634**, 109–127 (2005).
25. Dow-Hygelund, C. C. *et al.* UV continuum spectroscopy of a $6L^* z = 5.5$ galaxy. *Astrophys. J.* **630**, 137–140 (2005).
26. Yan, H. J. *et al.* The stellar masses and star formation histories of galaxies at $z \sim 6$: constraints from Spitzer observations in the Great Observatories Origins Deep Survey. *Astrophys. J.* (in the press); preprint at (<http://www.arXiv.org/astro-ph/0604554>) (2006).
27. Stark, D., Bunker, A. J., Ellis, R. S., Eyles, L. P. & Lacy, M. A new measurement of the stellar mass density at $z \sim 5$: implications for the sources of cosmic reionization. *Astrophys. J.* (submitted); preprint at (<http://www.arXiv.org/astro-ph/0604250>) (2006).
28. Spergel, D. *et al.* Wilkinson Microwave Anisotropy Probe (WMAP) three year results: implications for cosmology. *Astrophys. J.* (submitted); preprint at (<http://www.arXiv.org/astro-ph/0603449>) (2006).
29. Steidel, C. C., Adelberger, K. L., Giavalisco, M., Dickinson, M. & Pettini, M. Lyman-break galaxies at $z > \sim 4$ and the evolution of the ultraviolet luminosity density at high redshift. *Astrophys. J.* **519**, 1–17 (1999).
30. Schiminovich, D. *et al.* The GALEX-VVDS measurement of the evolution of the far-ultraviolet luminosity density and the cosmic star formation rate. *Astrophys. J.* **619**, 47–50 (2005).
31. Labbé, I., Bouwens, R. J., Illingworth, G. D. & Franx, M. Confirmation of *z*-dropout galaxies in the HUDF with Spitzer IRAC imaging: stellar masses and ages. *Astrophys. J.* (in the press); preprint at (<http://www.arXiv.org/astro-ph/0608444>) (2006).
32. Madau, P., Pozzetti, L. & Dickinson, M. The star formation history of field galaxies. *Astrophys. J.* **498**, 106–116 (1998).
33. Stanway, E. R., McMahon, R. G. & Bunker, A. J. Near-infrared properties of *i*-drop galaxies in the Hubble Ultra Deep Field. *Mon. Not. R. Astron. Soc.* **359**, 1184–1192 (2005).

Supplementary Information is linked to the online version of the paper at www.nature.com/nature.

Acknowledgements We are grateful to L. Bergeron, S. Kassin, D. Magee, M. Stiavelli, R. Thompson and A. Zirm for their help in reducing the NICMOS data, to M. Franx for critical reading of this manuscript, to S. Malhotra for making the NICMOS parallels to her PEARS program public early, and to I. Labbe for assistance in interpreting the IRAC data.

Author Information Reprints and permissions information is available at www.nature.com/reprints. The authors declare no competing financial interests. Correspondence and requests for materials should be addressed to R.J.B. (bouwens@ucolick.org).